Ndel1 suppresses ciliogenesis in proliferating cells by regulating the trichoplein–Aurora A pathway

Hironori Inaba,[1] Hidemasa Goto,[1,2] Kousuke Kasahara,[1,3] Kanako Kumamoto,[4] Shigenobu Yonemura,[6] Akihito Inoko,[1] Shotaro Yamano,[5] Hideki Wanibuchi,[5] Dongwei He,[1] Naoki Goshima,[7] Tohru Kiyono,[8] Shinji Hirotsune,[4] and Masaki Inagaki[1,2]

[1]Division of Biochemistry, Aichi Cancer Center Research Institute, Nagoya 464-8681, Japan
[2]Department of Cellular Oncology, Graduate School of Medicine, Nagoya University, Nagoya 466-8550, Japan
[3]Department of Oncology, Graduate School of Pharmaceutical Sciences, Nagoya City University, Nagoya 467-8601, Japan
[4]Department of Genetic Disease Research and [5]Department of Molecular Pathology, Osaka City University Graduate School of Medicine, Osaka 545-8585, Japan
[6]Center for Life Science Technologies (Ultrastructural Research Team), Institute of Physical and Chemical Research, Kobe 650-0047, Japan
[7]Molecular Profiling Research Center for Drug Discovery, National Institute of Advanced Industrial Science and Technology, Tokyo 135-0064, Japan
[8]Division of Carcinogenesis and Cancer Prevention, National Cancer Center Research Institute, Tokyo 104-0045, Japan

Primary cilia protrude from the surface of quiescent cells and disassemble at cell cycle reentry. We previously showed that ciliary reassembly is suppressed by trichoplein-mediated Aurora A activation pathway in growing cells. Here, we report that Ndel1, a well-known modulator of dynein activity, localizes at the subdistal appendage of the mother centriole, which nucleates a primary cilium. In the presence of serum, Ndel1 depletion reduces trichoplein at the mother centriole and induces unscheduled primary cilia formation, which is reverted by forced trichoplein expression or cok-nockdown of KCTD17 (an E3 ligase component protein for trichoplein). Serum starvation induced transient Ndel1 degradation, subsequent to the disappearance of trichoplein at the mother centriole. Forced expression of Ndel1 suppressed trichoplein degradation and axonemal microtubule extension during ciliogenesis, similar to trichoplein induction or KCTD17 knockdown. Most importantly, the proportion of ciliated and quiescent cells was increased in the kidney tubular epithelia of newborn Ndel1-hypomorphic mice. Thus, Ndel1 acts as a novel upstream regulator of the trichoplein–Aurora A pathway to inhibit primary cilia assembly.

Introduction

The primary cilium projects from the cell surface and is considered to function as a chemo- and/or mechanosensor (Singla and Reiter, 2006; Anderson et al., 2008; Gerdes et al., 2009; Nigg and Raff, 2009; Goetz and Anderson, 2010; Seeley and Nachury, 2010; Ishikawa and Marshall, 2011). Upon cell cycle exit, the mother centriole frequently gives rise to a basal body to nucleate a nonmotile and microtubule-rich protrusion ensheathed by the plasma membrane. Dysfunction of a primary cilium is associated with a broad spectrum of diseases such as polydactyly, craniofacial abnormalities, brain malformation, congenital heart diseases, situs inversus (defects of left–right patterning), obesity, diabetes, and polycystic kidney disease (Gerdes et al., 2009; Nigg and Raff, 2009; Li et al., 2015).

With the exception of some cells possessing primary cilia during cell proliferation, most cells begin to retract their primary cilia at the cell cycle reentry (Quarmby and Parker, 2005; Kim and Tsiokas, 2011; Goto et al., 2013). Forced induction of primary cilia can affect cell cycle progression (Kim et al., 2011; Li et al., 2011; Inoko et al., 2012), suggesting a possible checkpoint role for primary cilia in cell cycle progression. Recent studies have highlighted a mitotic kinase Aurora A as a negative regulator of primary cilia (Pugacheva et al., 2007; Kinzel et al., 2010; Inoko et al., 2012; Plotnikova et al., 2012). Several proteins were identified as Aurora A activators to disassemble primary cilia at cell cycle reentry (the G0/G1 transition; Pugacheva et al., 2007; Kinzel et al., 2010; Plotnikova et al., 2012) or inhibit their regeneration during cell proliferation (Inoko et al., 2012). Among them, trichoplein, a protein originally identified as a keratin intermediate filament scaffold protein (Nishizawa et al., 2005), localizes at mother and daughter centrioles in proliferating cells (Ibi et al., 2011). Trichoplein binds and activates Aurora A especially in G1 phase, which suppresses unscheduled primary cilia formation during cell proliferation (Inoko et al., 2012). As cells exit the proliferation cycle, trichoplein is polyubiquitinated at the mother centriole by Cul3-RING E3 ligase (CRL3)–KCTD17 complex (Kasahara

Correspondence to Masaki Inagaki: minagaki@aichi-cc.jp

Abbreviations used in this paper: CB, ciliary bud; CV, ciliary vesicle; Dox, doxycycline; MBP, maltose-binding protein; MT, microtubule; TEM, transmission electron microscopy; TPHD, trichohyalin and plectin homology domain.

The Rockefeller University Press $30.00
J. Cell Biol. Vol. 212 No. 4 409–423
www.jcb.org/cgi/doi/10.1083/jcb.201507046

et al., 2014). This CRL3^{KCTD17}-mediated trichoplein degradation enables quiescent cells to assemble primary cilia by limiting Aurora A activity (Kasahara et al., 2014).

Nuclear distribution element (NDE)-like 1 (Ndel1; also known as Nudel; Yamada et al., 2010; Chansard et al., 2011a; Bradshaw et al., 2013) was originally identified as a binding partner of Lis1, a dynein regulatory protein, from two-hybrid screening (Niethammer et al., 2000). Because Ndel1 also interacts with dynein and modifies its activity, Ndel1 is considered to regulate microtubule (MT) dynamics and MT-based transport (Sasaki et al., 2000; Liang et al., 2004; Vergnolle and Taylor, 2007; Yamada et al., 2008; Zyłkiewicz et al., 2011). Numerous proteins have been identified as Ndel1-binding partners including kinases, ATPases and GTPases, some activities and functions of which are modulated by the interaction with Ndel1 (Kim et al., 2009; Mori et al., 2009; Bradshaw et al., 2011; Chansard et al., 2011b). Therefore, Ndel1 is known as a scaffold protein involved in numerous cellular processes such as mitosis, neuronal development, and neuronal migration (Yamada et al., 2010; Chansard et al., 2011a; Bradshaw et al., 2013). Here, we have unexpectedly identified Ndel1 as a suppressor of primary cilia assembly likely through the stabilization of trichoplein at the mother centriole.

Results

Ndel1 knockdown induces unscheduled primary cilia formation

By searching a public database (Human Gene and Protein Database, http://www.HGPD.jp), we found that 77 proteins including trichoplein possess putative trichohyalin and plectin homology domain (TPHD; Nishizawa et al., 2005; Table S1). A comprehensive siRNA screen for TPHD-containing proteins revealed that four proteins might show ciliary phenotypes similar to trichoplein (Inoko et al., 2012; unpublished data; Fig. 1, B and C). Here, we focused on Ndel1 (Yamada et al., 2010; Chansard et al., 2011a; Bradshaw et al., 2013; Fig. S1 A). To examine Ndel1 localization, we stained HeLa (human cervical carcinoma) and RPE1 (h-TERT–immortalized retinal pigment epithelia) cells with appropriate markers, together with anti-Ndel1 (Fig. 1 A and Fig. S1, B and C). Ndel1 was diffusely localized in the cytoplasm but concentrated in the centrosome (Fig. S1 B and Fig. 1 A, magnified images). Ndel1 localized at proximal sites of CEP164, a marker of distal appendage on the mother centriole (Graser et al., 2007; also see the bottom of merged images with cartoons in Fig. 1 A). Anti-ninein signals were detected as four dots (Figs. 1 A and S1 C), supporting previous studies that ninein was localized not only at subdistal appendages of the mother centriole but also at the proximal ends of both centrioles (Mogensen et al., 2000; Ou et al., 2002; Delgehyr et al., 2005). Anti-Ndel1 signals closely overlapped with two dots of anti-ninein signals: Ndel1 appeared to exist inside subdistal appendage-associated ninein. As shown in Fig. S1 C, anti-Ndel1 signals partially overlapped with Odf2 (a protein of distal/subdistal appendages on the mother centriole; Lange and Gull, 1995; Nakagawa et al., 2001; Ishikawa et al., 2005) or centrin 2 (a protein at the distal ends of centrioles; Paoletti et al., 1996; Laoukili et al., 2000). These results suggested that Ndel1 localizes at the subdistal appendage of mother centriole, which is consistent with a previous study (Guo et al., 2006).

Because Odf2 (Lange and Gull, 1995; Nakagawa et al., 2001; Ishikawa et al., 2005) or ninein (Mogensen et al., 2000; Ou et al., 2002; Delgehyr et al., 2005) was reportedly localized at the subdistal appendage, we analyzed the relationship between Ndel1 and Odf2/ninein. Ndel1 localization was impaired by Odf2 depletion in HeLa cells, whereas Ndel1 depletion did not affect Odf2 localization (Fig. S2, A and B). Because Odf2 is essential for distal and subdistal appendage formation on the mother centriole (Tateishi et al., 2013), the presence of a subdistal appendage may be required for Ndel1 targeting to centrosome. However, neither ninein nor Ndel1 knockdown affected their mutual localization (Fig. S2, C and D). To address functional consequences of their depletion by RNAi, we performed a MT-regrowth assay after cold depolymerization (Dammermann and Merdes, 2002; Delgehyr et al., 2005; Ibi et al., 2011; Fig. S2 E). Similar to control cells, Ndel1-depleted cells assembled an extensive array of cytoplasmic MTs that were centered at the centrosome at 5 min after warming. In contrast, this radial, centrosome-based organization was severely impaired by ninein knockdown, supporting the importance of ninein in MT anchoring as reported previously (Dammermann and Merdes, 2002; Delgehyr et al., 2005; Ibi et al., 2011). Therefore, Ndel1 may function independently of ninein at the subdistal appendage of mother centriole.

To confirm our siRNA data (unpublished data), we stained transfected RPE1 cells with anti–acetylated tubulin and anti-Ndel1 48–72 h later. Ndel1 knockdown led to increased number of cells with a linear object that stained with anti–acetylated tubulin and protruded from the cell surface (Fig. 1, B and C). Transmission electron microscopy (TEM) analysis verified this structure as a primary cilium, characterized by the presence of membranous sheaths surrounding the axonemal MTs and a clear structural transition between the basal body and the cilium (Fig. 1 D). Using electron microscopy, we also detected electron-dense, appendage-like structures in Ndel1-depleted, ciliated cells (Fig. 1 D). In addition, Ndel1 depletion did not affect the localization of appendage proteins even in the ciliated cells (Fig. 1 E). These results suggested that Ndel1 depletion induced unscheduled primary ciliary assembly without affecting appendage structures.

The human *NDEL1* gene gives rise to two splice variants (isoforms A and B; Fig. S3 A). Deletion of amino acids 256 to 291 (Δ256–291; Fig. S3 A) from the isoform B splice variant inhibited its localization at the centrosome (Liang et al., 2004). We established three types of RPE1 cell lines allowing the expression of each Ndel1 not only tagged with a C-terminal myc-epitope but also possessing silent mutations to resist each siNdel1-mediated knockdown in a doxycycline (Dox)-dependent manner. Unscheduled cilia formation caused by siNdel1 RNAs (target sequence 2 or 3) was reverted by Dox-induced expression of Ndel1 isoform A or B (Fig. S3, B–D). Therefore, the ciliary phenotype was caused by the reduction of Ndel1 protein level regardless of the isoform. Because Dox-induced expression of Δ256–291 did not revert the ciliary phenotype induced by Ndel1 knockdown (Fig. S3, B–D), it was hypothesized that centrosomal targeting of Ndel1 is required for the suppression of unscheduled cilia formation in proliferating cells. Based on these results (Fig. S3), we focused on Tet-On RPE1 cells expressing the myc-tagged Ndel1 isoform B (called Ndel1-Myc) in subsequent experiments. Because Ndel1-Myc induction improved unscheduled cilia formation by the transfection with each siNdel1 (target sequence 1, 2, or 3; Fig. 1, F–H; and Fig. S3, B–D), we used either of three siRNAs for the following Ndel1 knockdown in RPE1 cells. The results suggested that

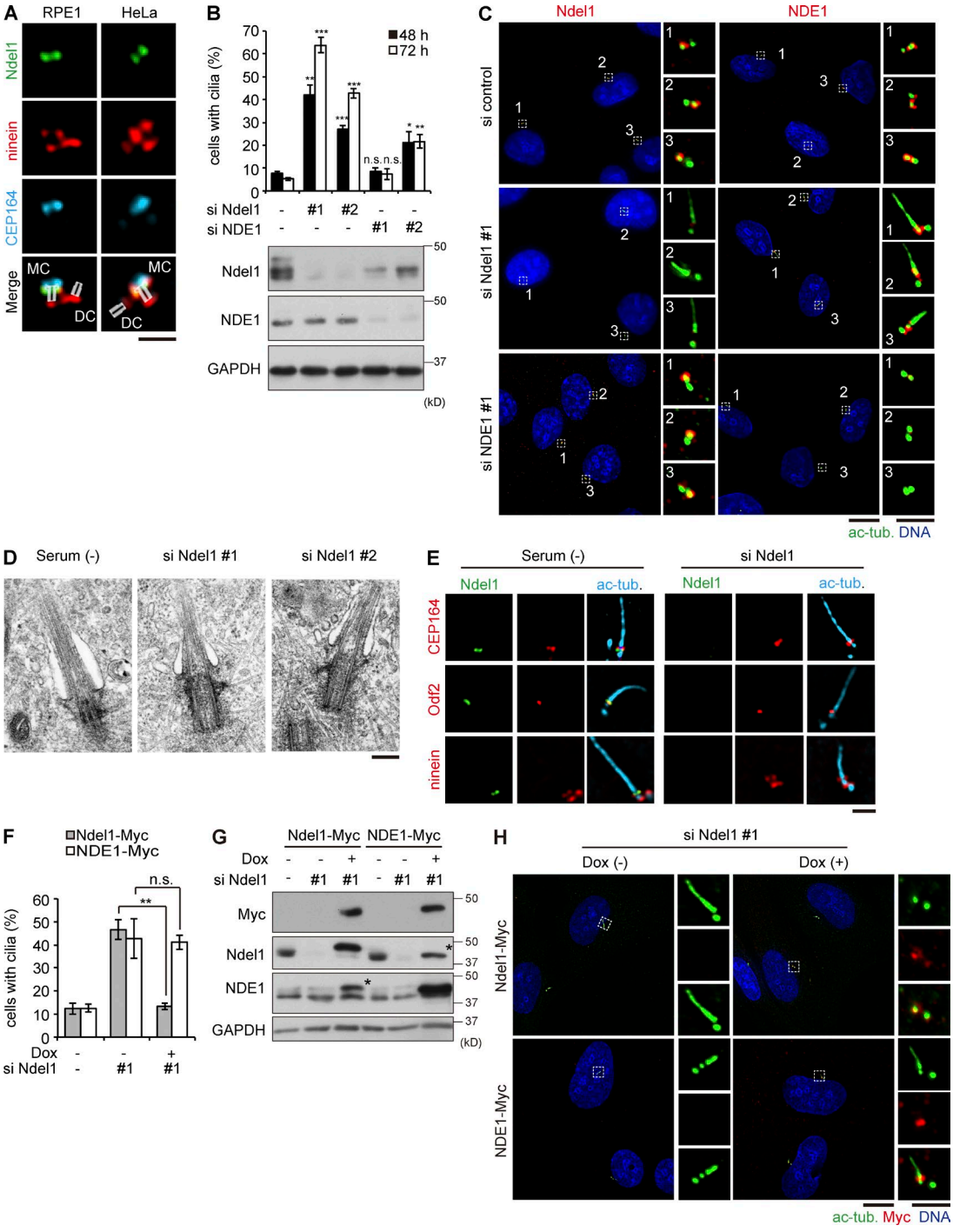

Figure 1. **Ndel1 localizes at subdistal appendages of centrioles and suppresses unscheduled primary cilia assembly in proliferating RPE1 cells.** (A) Ndel1 localization at the centrosome. RPE1 or HeLa cells were stained with the indicated antibodies. Each merged image is shown with cartoons; MC and DC indicate a mother centriole (possessing distal and subdistal appendages at the distal end) and a daughter centriole (without appendages), respectively. The entire cell images are shown in Fig. S1 B. (B–H) Proliferating RPE1 cells were transfected with each Ndel1- or NDE1-specific siRNA (target sequence 1 or 2) or control siRNA. For rescue experiments (F–H), we used RPE1 cells expressing Ndel1 isoform B (see Fig. S3 A) or NDE1 with C-terminal myc tag and silent mutations (to resist siRNA-mediated Ndel1 knockdown; Ndel1-Myc or NDE1-Myc) in a doxycycline (Dox)-dependent manner. 4 h after the transfection, the medium was changed to a new growing medium with (+) or without (–) 3 ng/ml Dox. The cells were collected at 48 (B–H) or 72 (B) h after transfection for the following analyses. The siRNA-treated cells were subjected to the immunoblotting (B and G), the immunostaining (B, C, E, F, and H) or TEM (D). GAPDH was used as a loading control (B and G). Asterisks indicate nonspecific bands caused by overproduction (G). Insets show magnified images of indicated centrosomes in lower micrographs (C and H). As control ciliated cells, we incubated RPE1 cells in the serum-free medium for 48 h (serum [–] in D and E). Exogenous Ndel1 or NDE1 was detected with anti-Myc antibody (F–H). Based on immunostaining patterns of anti–acetylated tubulin (ac-tub; C and H), we calculated the percentage of ciliated cells (B and F). Data represent mean ± SEM of three independent experiments ($n > 100$ each). *, $P < 0.05$; **, $P < 0.01$; and ***, $P < 0.001$, two-tailed unpaired Student's *t* test. Bars: (A and E) 1 µm; (C and H, main) 5 µm; (C and H, insets) 1 µm; (D) 0.2 µm.

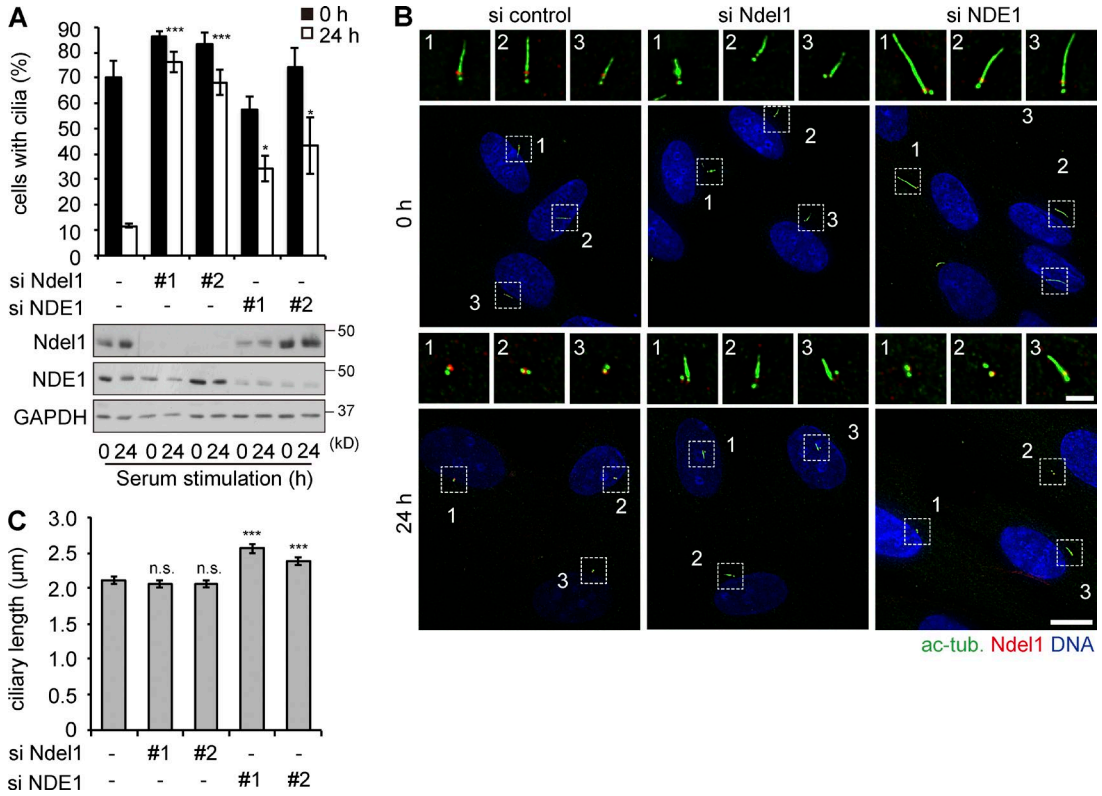

Figure 2. **Ndel1 is required for deciliation at cell cycle reentry.** To evaluate deciliation at the cell cycle reentry, RPE1 cells were incubated in serum-free media from 24 to 72 h after the transfection and then cultured in the presence of 10% serum for 0 or 24 h (Time after serum stimulation). Based on immunostaining of anti–acetylated tubulin (ac-tub.), we measured the length of primary cilia before serum stimulation (for 48 h serum starvation, C). The data are shown as mean ± SEM from three independent experiments (n > 100 each in A or n = 40 each in C). Bars: (main) 5 µm; (insets) 1 µm.

Ndel1 exerts its inhibitory effect on ciliogenesis in proliferating cells, a function similar to trichoplein (Inoko et al., 2012).

Functional correlation of Ndel1 with NDE1, Lis1, or dynein

NDE1 (also known as NudE) is highly similar to Ndel1 at the amino acid sequence level (Bradshaw et al., 2013). These paralogous proteins share some common functions (Bradshaw et al., 2013). Like Ndel1, NDE1 localized to the subdistal appendages, whereas neither NDE1 nor Ndel1 knockdown affected their mutual localization (Fig. 1 C). One NDE1-specific siRNA (target sequence 2) slightly increased the proportion of ciliated cells, whereas the other siRNA (target sequence 1) displayed no significant increase (Fig. 1, B and C). Thus, with regard to the suppression of ciliogenesis in proliferating cells, NDE1 participation was only marginal at best. In addition, unscheduled cilia formation caused by Ndel1 depletion was not reverted by Dox-induced expression of NDE1 (Fig. 1, F–H), suggesting that NDE1 expression may not compensate for Ndel1 loss.

Because NDE1 was reportedly required for deciliation at cell cycle reentry (Kim et al., 2011), we examined whether Ndel1 exerts the same function. The cells were treated with each siRNA for 24 h, followed by serum-free medium for 48 h and finally in serum-containing medium for the indicated time (Fig. 2). As reported previously (Kim et al., 2011), NDE1 depletion delayed deciliation process (Fig. 2, A and B). The delay was also observed in Ndel1-depleted cells (Fig. 2, A and B). Thus, both proteins participate in the deciliation processes when cells reenter the cell cycle.

Because NDE1 is also known to regulate ciliary length (Kim et al., 2011), we measured the length, using RPE1 cells cultured without serum for 48 h (Fig. 2 C; also see magnified micrographs at 0 h in Fig. 2 B). NDE1-depleted cells had longer cilia than control cells. In contrast, we observed no significant differences between control and Ndel1-depleted cells.

Because Ndel1 interacts with Lis1 (Niethammer et al., 2000), we examined the effects of Lis1 depletion. Lis1 knockdown not only induced unscheduled ciliary assembly (Fig. 3, A and B) but also increased the distance between nucleus and centrosome (Fig. 3 C); the latter phenotype was previously reported in *LIS1*$^{+/-}$ neurons (Tanaka et al., 2004). However, no apparent phenotypes of nucleus–centrosome coupling were observed in Ndel1-depleted cells (Fig. 3 C). Lis1 depletion delayed deciliation process at cell cycle reentry, like Ndel1 depletion (Fig. 3 D).

We next examined the effects of cytoplasmic dynein 1 heavy chain 1 (DYNC1H1) and intermediate chain 2 (DYNC1I2), because Ndel1, NDE1, and Lis1 interact with dynein and modulate its activity (Yamada et al., 2010; Chansard et al., 2011a; Bradshaw et al., 2013). The knockdown of DYNC1H1 (Fig. 3, E and F) or DYNC1I2 (Fig. 3, H and I) might increase the proportion of ciliated cells under cultivation with serum, but the effects were if at all only marginal. In contrast, deciliation process after serum addition was significantly delayed by the treatment with each DYNC1H1 (Fig. 3 G) or DYNC1I2 siRNA (Fig. 3 J), except for one DYNC1I2 siRNA (target sequence #1; Fig. 3 J). Cytoplasmic dynein 2 heavy chain 1 depletion exhibited similar tendency in the two assays (unpublished data; Fig. 3, E–J).

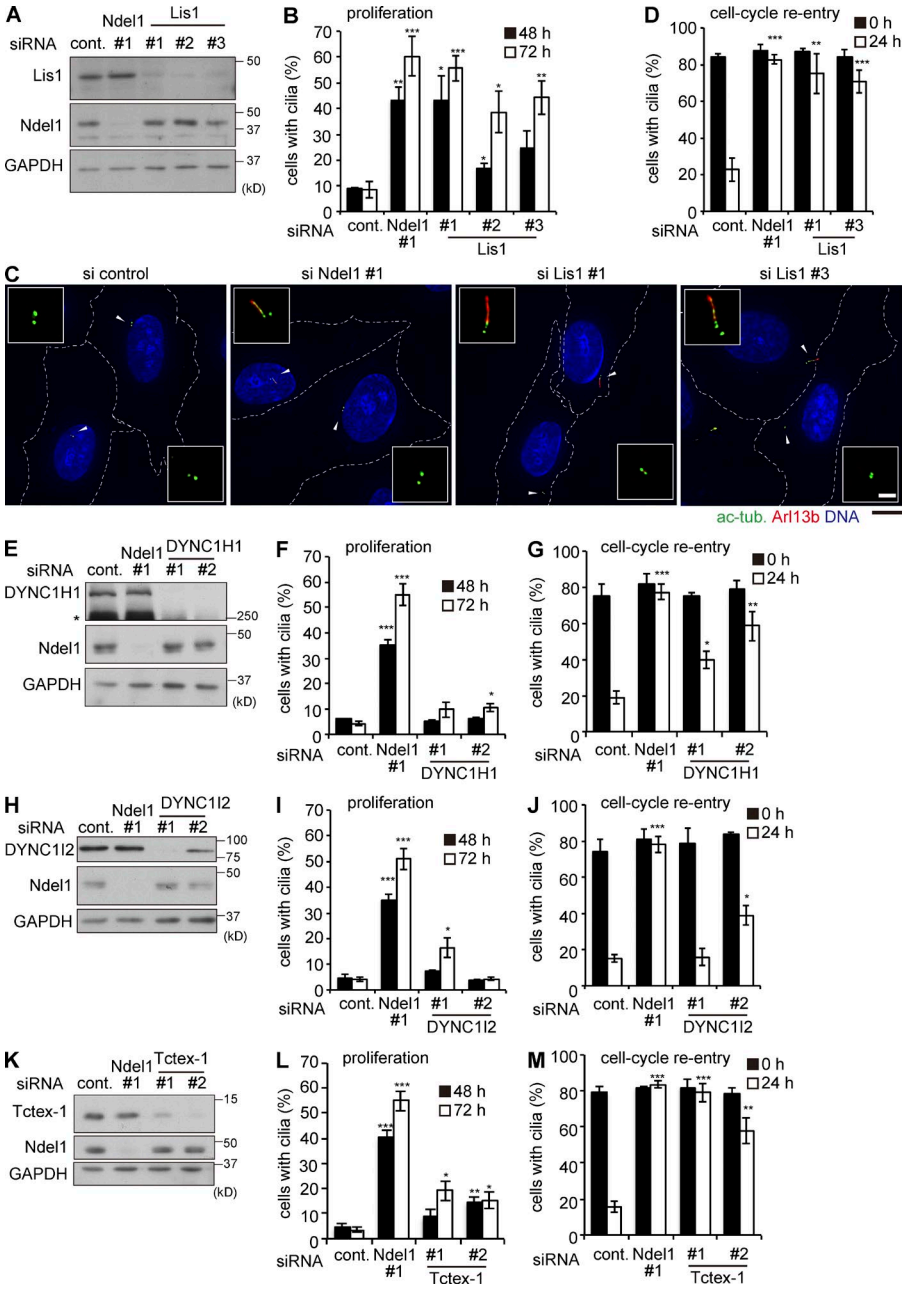

Figure 3. **Comparison of ciliary phenotypes among Ndel1, NDE1, Lis1, and dynein.** RPE1 cells were treated with Ndel1-, Lis1- (A–D), DYNC1H1- (E–G), DYNC1I2- (H–J), or Tctex-1–specific (K–M) siRNA. We evaluated unscheduled ciliation in proliferating cells (A–C, E, F, H, I, K, and L) or deciliation at cell cycle reentry (D, G, J, and M) as described in the legends of Figs. 1 or 2, respectively. The data are shown as mean ± SEM from three independent experiments (n > 100 each). White arrowheads indicate centrosome or primary cilia; these images were magnified in insets. White dashed line indicates cell borders. Asterisk indicates degraded products (E). Bars: (main) 5 µm; (insets) 1 µm. ac-tub., anti–acetylated tubulin.

Because dynein light-chain Tctex-type 1 (Tctex-1) was reported to participate in the deciliation process (Li et al., 2011) and control ciliary length (Palmer et al., 2011), we further examined the effects of Tctex-1 knockdown on ciliary dynamics. Tctex-1 depletion elevated the proportion of ciliated cells under cultivation with serum, but the effect was much weaker compared with Ndel1 depletion (Fig. 3, K and L). Meanwhile, Tctex-1 depletion delayed the deciliation process after serum addition (Fig. 3 M) as reported previously (Li et al., 2011).

Collectively, Ndel1, NDE1, Lis1, and dynein complexes participate in ciliary absorption at cell cycle reentry (Fig. 2 and Fig. 3, D, G, J, and M; Kim et al., 2011; Li et al., 2011). NDE1 (Fig. 2 C; Kim et al., 2011), Lis1 (unpublished data), and dynein complexes (Palmer et al., 2011) negatively regulate ciliary length in quiescent RPE1 cells, whereas Ndel1 is unlikely to share this function (Fig. 2 C). In addition, Ndel1 and Lis1 suppress unscheduled cilia formation in proliferating cells, whereas NDE1 and dynein complexes only marginally contributed this process.

Ndel1 depletion induces cilia-dependent cell cycle arrest

We examined the effect of Ndel1 depletion on cell cycle progression in RPE1 cells in the presence of serum. Staining for cyclin A as a marker for the transition of G1/S to pro(meta) phase (Murray, 2004) revealed that Ndel1 depletion reduced both the proportion of cyclin A–positive cells (Fig. 4, A and B) and the protein level of cyclin A (Fig. 4 C). Pulse-labeling experiments using BrdU also demonstrated that Ndel1 knockdown reduced the number of proliferating cells (Fig. 4 D). FACS analysis showed that Ndel1 depletion increased the percentage of cells with 2N DNA content (Fig. 4, E and F). These results suggested that Ndel1 depletion induces cell cycle arrest at the G0/G1 phase.

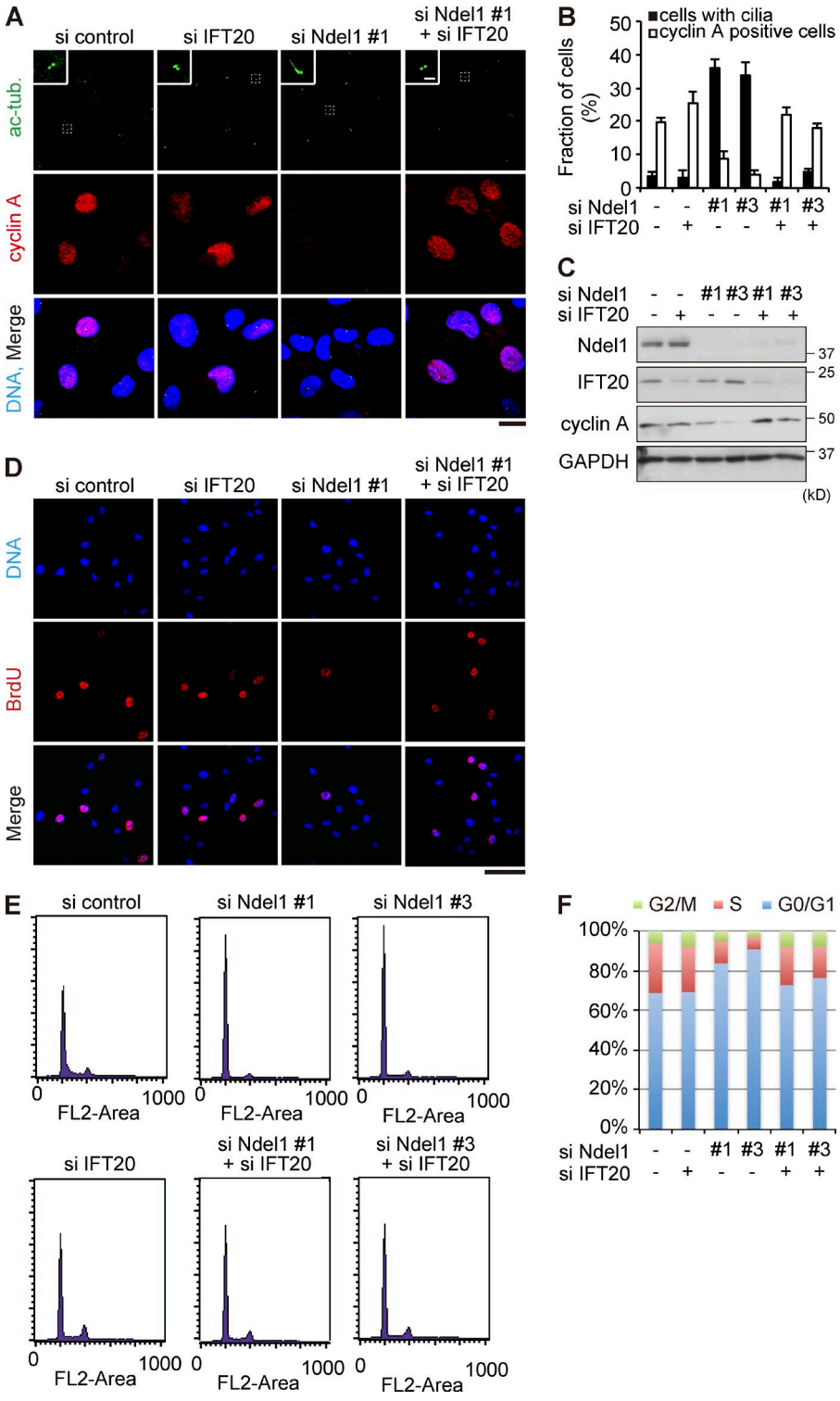

Figure 4. **Ndel1 knockdown causes primary cilium-dependent cell cycle arrest.** (A–F) Proliferating RPE1 cells were treated with the combination of the indicated siRNA(s) as reported previously (Inoko et al., 2012). The treated cells were subjected to immunostaining (A, B, and D), immunoblotting (C), or FACS analysis (E and F). Insets show magnified images of indicated centrosomes in lower micrographs (A). The data are shown as mean ± SEM from three independent experiments ($n > 100$ each in B). BrdU (D) and FACS (E and F) analyses were performed as described previously (Inoko et al., 2012). Data from a single representative sample are shown (D and E). Bars: (A, main images) 10 µm; (A, insets) 1 µm; (D) 50 µm.

Because IFT20 is essential for ciliogenesis (Follit et al., 2006), we analyzed the effect of IFT20 coknockdown. With regard to ciliary formation, the effect of Ndel1 knockdown was alleviated by IFT20 coknockdown (Fig. 4, A and B). This restored cell proliferation to almost normal levels, based upon the analysis of several cell markers (Fig. 4). In contrast, single knockdown of IFT20 had little impact on cell cycle progression (Fig. 4). Therefore, in Ndel1-depleted cells, the cell cycle arrest is mediated by the formation of an unscheduled primary cilium, similar to trichoplein-depleted cells (Inoko et al., 2012).

Ndel1 induction suppresses primary cilia formation in response to serum starvation

Using RPE1 cells, we examined the behavior of Ndel1 after serum starvation. Ndel1 protein levels were reduced 4 to 24 h after serum depletion (Fig. 5, A and B). This was accompanied by decreased Ndel1 staining at the centrosome for ∼24 h after the starvation (Fig. 5, C and D). Treatment with protease inhibitors restored Ndel1 protein levels almost completely (Fig. 5 E), indicating that serum depletion caused the reduction in Ndel1 protein levels by protein degradation. Interestingly, the time

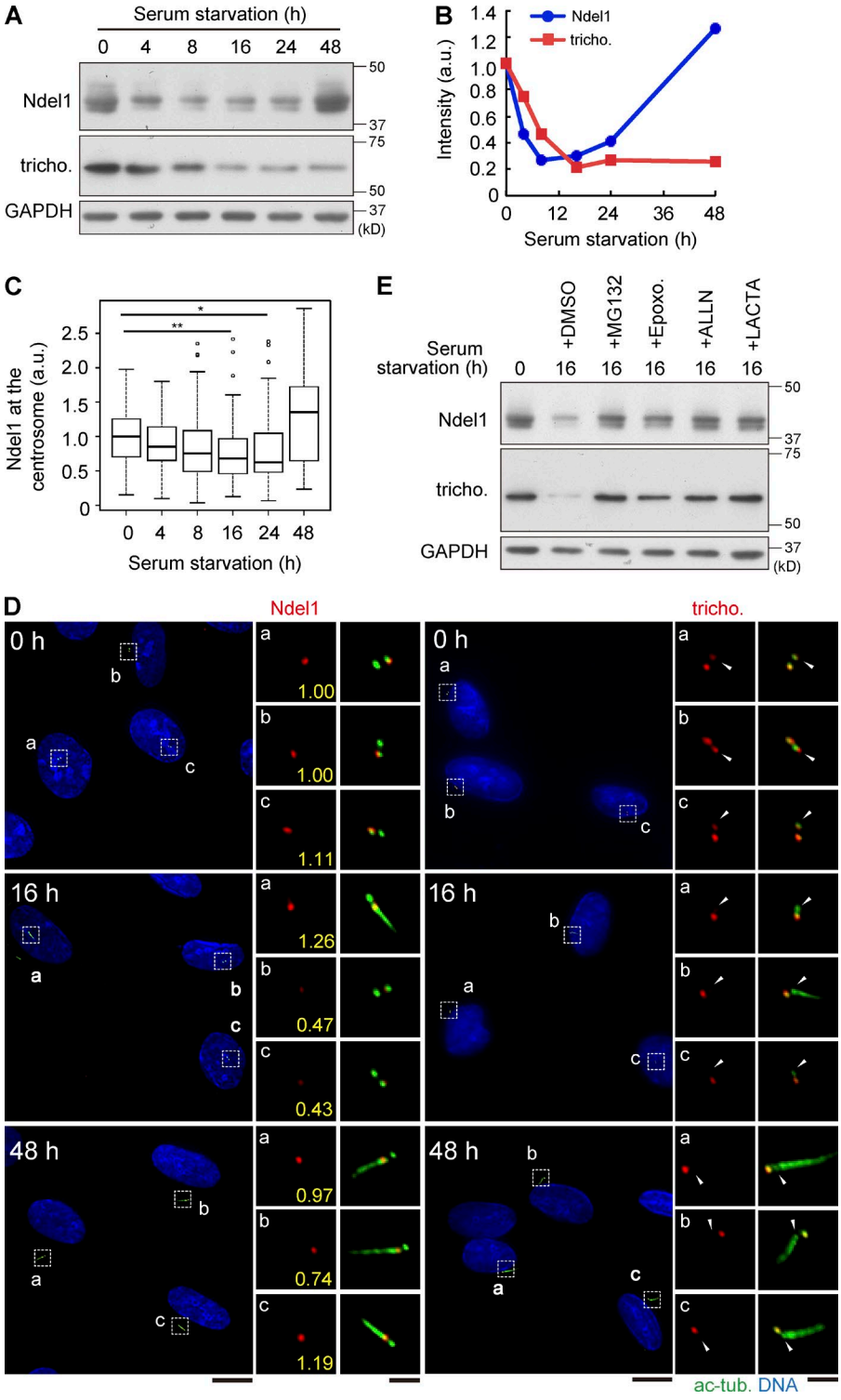

Figure 5. **Ndel1 is transiently degraded via ubiquitin-proteasome pathway in response to serum starvation.** (A–D) RPE1 cells were cultured in the serum-free medium for the indicated time. The treated cells were subjected to immunoblotting (A and B) or immunostaining (C and D). In B, the amount of Ndel1 and trichoplein (tricho.; A) was quantified using densitometry, normalized to the content of GAPDH (A), and presented as fold of 0 h (data are shown from a single representative sample; Li et al., 2012). In C, the cells were stained with anti–centrin-2 (a centriolar marker) and anti-Ndel1 antibodies. Judging by the anti–centrin-2 staining pattern, we selected cells possessing two centrioles per cell (implying cells before centrosome duplication) and then quantified fluorescence intensity of anti-Ndel1 signals at the centrosome (box-and-whisker plots; $n = 60$ from three independent experiments in C) as described previously (Kasahara et al., 2014). Relative intensity of centriole-associated Ndel1 is indicated in yellow (D, left). Arrowheads indicate the position of mother centriole (D, right). (E) RPE1 cells were cultured in the serum-free medium containing 5 µM MG132, 50 nM Epoxomicin (Epox), 10 µM ALLN, or 3 µM Lactacystin (Lacta) for 16 h. We used the equal volume of DMSO as a negative control. Bars: (main) 5 µm; (insets) 1 µm.

course of degradation appears to differ between trichoplein and Ndel1. Trichoplein was decreased at a slower rate and remained at low levels after serum starvation (Fig. 5, A and B). As reported previously (Kasahara et al., 2014), serum depletion results in the disappearance of trichoplein at the mother centrioles (Fig. 5 D, arrowheads). In contrast, Ndel1 protein levels were initially reduced but recovered ∼48 h after serum starvation (Fig. 5, A and B). Immunocytochemical analyses also revealed that centrosome-associated Ndel1 was decreased after serum depletion but recovered after cilia formation (Fig. 5, C and D). Because Ndel1-Myc induction by Dox decreased the proportion of ciliated cells in the absence of serum (Fig. 6 A), transient Ndel1 degradation is required for ciliary assembly, at least in the absence of serum.

Ndel1 protects trichoplein from CRL3^{KCTD17}-mediated degradation at the mother centriole

We examined the relationship between Ndel1 and trichoplein. Ndel1-Myc induction by Dox recovered not only trichoplein

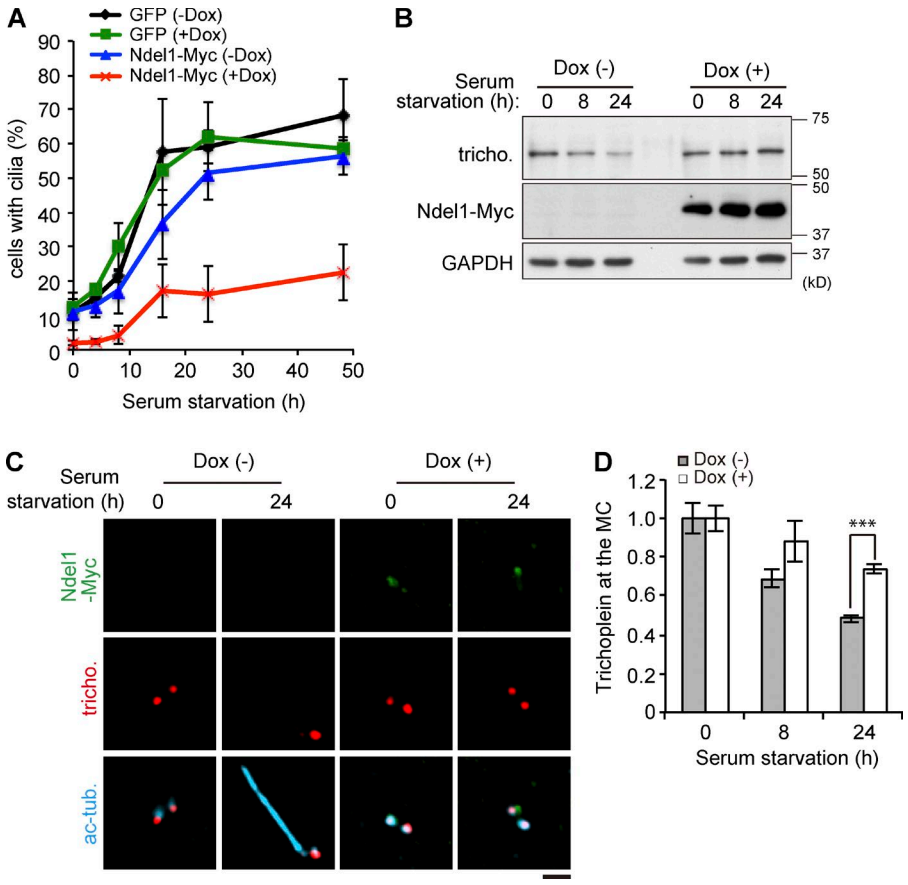

Figure 6. **Exogenous Ndel1 expression inhibits primary cilia assembly in serum-starved cells.** (A–D) Tet-On RPE1 cell line expressing inducible GFP (A) or Ndel1-Myc (A–D) was incubated with (+) or without (–) 30 ng/ml Dox in the growing medium for 24 h and then in the serum-free medium for the indicated time. Treated cells were subjected to immunostaining (A, C, and D) or immunoblotting (B). In A, the percentage of ciliated cells was quantified as described in the legend of Fig. 1. As judged by the immunostaining data (C), the proportion of cells with a trichoplein-positive mother centriole (MC) was quantified and normalized to 0 h after serum starvation in each group, which was set at 1.0. The data are shown as mean ± SEM from three independent experiments (n > 100 each; A and D). Bar, 1 µm.

protein levels (Fig. 6 B) but also its association with the mother centriole (Fig. 6, C and D) in serum-starved cells. In contrast, Dox-induced expression of maltose-binding protein (MBP)-trichoplein-Flag (Inoko et al., 2012) had little impact on transient Ndel1 degradation in response to serum depletion (Fig. 7 A). Thus, Ndel1 degradation likely has to precede trichoplein degradation during the course of ciliogenesis.

Conversely, Dox-mediated induction of MBP-trichoplein-Flag (Ibi et al., 2011) rescued the unscheduled primary cilia formation induced by Ndel1 depletion in the presence of serum (Fig. 7 B). Meanwhile, Ndel1-Myc induction did not compensate for trichoplein depletion (Fig. 7 C). Because trichoplein binds and activates Aurora A (Inoko et al., 2012), we examined the effect of Ndel1 knockdown on the level of Aurora A phosphorylated at Thr288 (Aurora A–pT288), which implies an active form of Aurora A. As shown in Fig. 7 D, Ndel1 depletion reduced Aurora A–pT288 level, like trichoplein depletion (Inoko et al., 2012). Because trichoplein is polyubiquitinated by $CRL3^{KCTD17}$ and then degraded specifically at the mother centriole (Kasahara et al., 2014), we performed a KCTD17 knockdown. KCTD17 codepletion alleviates both Aurora A–pT288 reduction and unscheduled ciliation by the knockdown of Ndel1, but not by the knockdown of trichoplein (Fig. 7 D). Ndel1 knockdown also reduced mother-centriole–associated trichoplein, and this effect was also reversed by KCTD17 co-knockdown (Fig. 7 E). Because the KCTD17 knockdown itself had little impact on both Ndel1 protein levels (Fig. 7 D) and centrosome-associated Ndel1 (Fig. 7 E), it is unlikely that Ndel1 degradation is directly regulated by $CRL3^{KCTD17}$. It rather suggests that Ndel1 likely protects mother-centriole–associated trichoplein from $CRL3^{KCTD17}$-mediated degradation, resulting in Aurora A activation.

Ndel1 suppresses axonemal extension during ciliogenesis

Ciliogenesis is a multistep process (Sorokin, 1968; Molla-Herman et al., 2010). Cytoplasmic vesicles dock to the distal appendage of mother centriole/basal body (step 1a) and then fuse with each other to form ciliary vesicle (CV; step 1b); electron-dense materials, termed the ciliary bud (CB), accumulate at the distal ends of a basal body (just beneath the CV; step 2); MTs start to elongate from a basal body and then form the axonemal shaft and the ciliary pocket (step 3); the CV finally fuses with plasma membrane before or after step 3 and the cilium emerges into the extracellular environment (see the cartoon [Kasahara et al., 2014] in Fig. S4 A). In serum-starved cells expressing Ndel1-Myc, CVs docked to distal appendages on mother centrioles in most cells (9 out of 11), some of which (5 out of 11) also formed the CB (Figs. 8 A and S4). However, the induction of Ndel1-Myc by Dox prevented the majority of serum-starved cells from proceeding to the step 3 in ciliogenesis (Figs. 8 A and S4). In the aforementioned experimental condition, exogenous Ndel1-Myc properly localized to the centrosome (i.e., subdistal appendage) and cytoplasm (Fig. 8 B) as an endogenous protein (Figs. 1 A and S1 B). Similar disturbance of ciliation steps was induced by exogenous trichoplein expression (Fig. 8 A) or KCTD17 knockdown (Kasahara et al., 2014). Therefore, Ndel1 negatively regulates axonemal extension during ciliogenesis by stabilizing trichoplein at the mother centriole (Fig. 8 C).

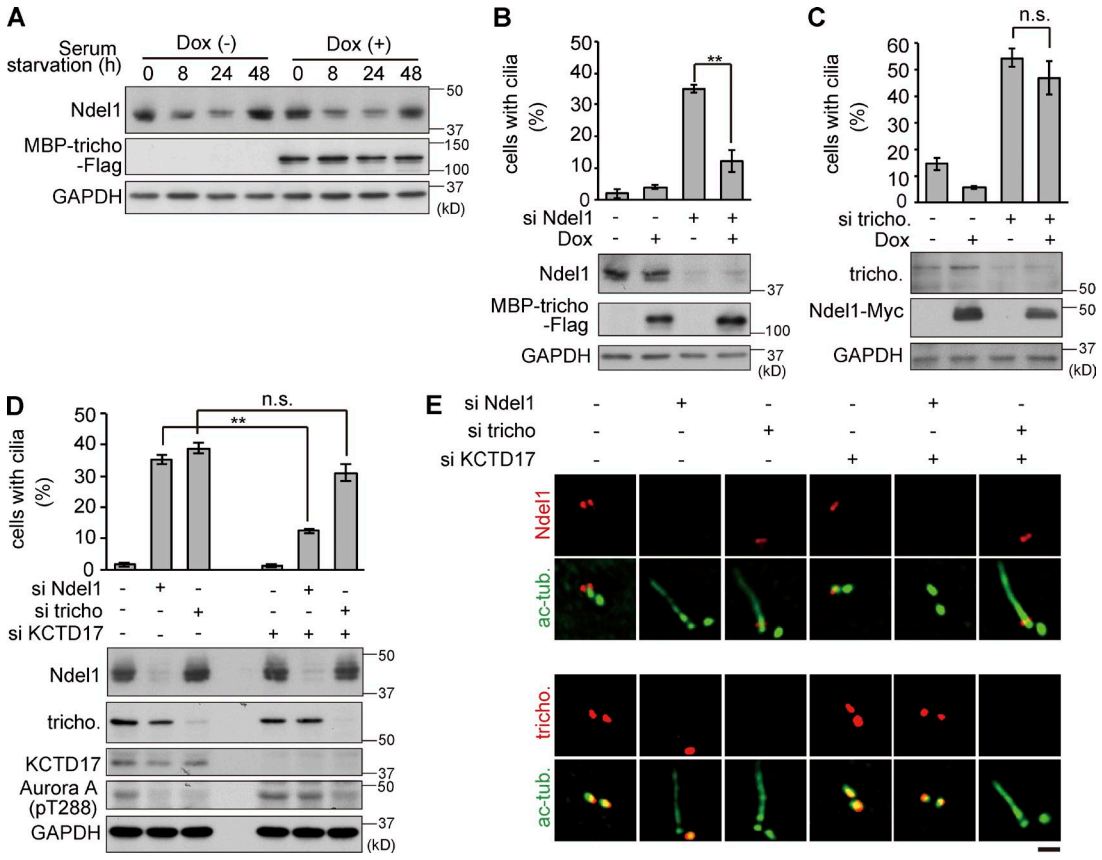

Figure 7. **Primary cilia assembly by Ndel1 depletion is reverted by trichoplein overproduction or KCTD17 coknockdown.** (A) Tet-On RPE1 cell line expressing inducible MBP-trichoplein-Flag (MBP-tricho-Flag) was incubated with (+) or without (–) 100 ng/ml Dox in the growing medium for 16 h and then in the serum-free medium for the indicated time. (B and C) Tet-On RPE1 cells were transfected with the indicated siRNA. 6 h after transfection, the cells were incubated with (+) or without (–) Dox for an additional 42 h. (D and E) Proliferating RPE1 cells were treated with combination of the indicated siRNA(s) for 48 h. The graph in D indicates the percentage of ciliated cells; n.s., not significant. The data are shown as mean ± SEM from three independent experiments (n > 100 each). Bar, 500 nm.

Reduced expression of Ndel1 increases the proportion of ciliated and Ki-67–negative cells in the kidney tubular epithelia of newborn mice

Because *NDEL1* knockout mice were reported to be embryonic lethal (Sasaki et al., 2005), we analyzed mice with low levels of Ndel1 expression (*NDEL1*$^{cko/cko}$; Fig. 9 A; Sasaki et al., 2005) to elucidate Ndel1 function in vivo. *NDEL1*$^{cko/cko}$ mice exhibited abnormalities in telencephalon development and hippocampus pyramidal cell morphology (Sasaki et al., 2005). We also found obesity in *NDEL1*$^{cko/cko}$ male mice (Fig. 9, B and C). Because obesity is frequently observed in cilia-related diseases (Gerdes et al., 2009; Nigg and Raff, 2009; Li et al., 2015), we analyzed newborn kidney. To that end, histological sections of proximal and distal tubules and collecting ducts in the kidney of control newborn mice (*NDEL1*$^{WT/WT}$; Fig. 9 D) were compared with *NDEL1*$^{cko/cko}$ at postnatal day 0. This revealed three major abnormalities in the latter. First, *NDEL1*$^{cko/cko}$ increased the proportion of ciliated cells in proximal tubules compared with *NDEL1*$^{WT/WT}$ (Fig. 9, E and F). Second, cilia were longer in proximal and distal tubules and collecting ducts of *NDEL1*$^{cko/cko}$ (Fig. 9, E and G). Third, judged by anti–Ki-67 staining, proliferating cells were decreased in tubular epithelia of *NDEL1*$^{cko/cko}$ kidney (Fig. 9, H and I). Thus, the increase of ciliated and quiescent cells in the kidney of newborn *NDEL1*$^{cko/cko}$ confirmed the observations made with RPE1 cells based on RNAi against Ndel1 (Figs. 1 and 4).

Using serum-starved RPE1 cells, we observed only marginal differences in ciliary length between control and Ndel1 knockdown (Fig. 2, B and C). Less than 10% of proliferating RPE1 cells had primary cilia (e.g., Fig. 1 B). However, in newborn kidney, ∼70–90% cells had cilia (Fig. 9, E and F), whereas ∼30% cells were proliferating (Fig. 9, H and I). Thus, not a few proliferating cells were assumed to possess primary cilia. Thus, we used another cell line, Swiss 3T3 (mouse fibroblast), because ∼50% of Swiss 3T3 cells possessed primary cilia under the cultivation with serum (Fig. 10 A). For mouse Ndel1 knockdown, we use a siRNA specific to mouse Ndel1 (target sequence m1) in addition to siNdel1 3 (the target sequence of which is completely conserved between human and mouse Ndel1). In Swiss 3T3 cells, Ndel1 depletion induced only marginal changes in the percentage of ciliated cells under cultivation with serum (Fig. 10 A). This observation was in contrast to results obtained in RPE1 cells (e.g., Fig. 1 B), which was likely caused by the difference in ciliary dynamics during cell proliferation (i.e., Swiss 3T3 cells form cilia under the cultivation with serum). Next, we analyzed the effect on quiescent Swiss 3T3 cells. As shown in Fig. 10 B, Ndel1-Myc induction by Dox inhibited ciliation in Swiss 3T3 cells, like RPE1 cells (Fig. 6 A), suggesting that Ndel1 also functions as a negative regulator of cilia formation in quiescent Swiss 3T3 cells. Meanwhile, Ndel1 knockdown lengthened the primary cilia during quiescent state (Fig. 10, C–E). Therefore, Ndel1

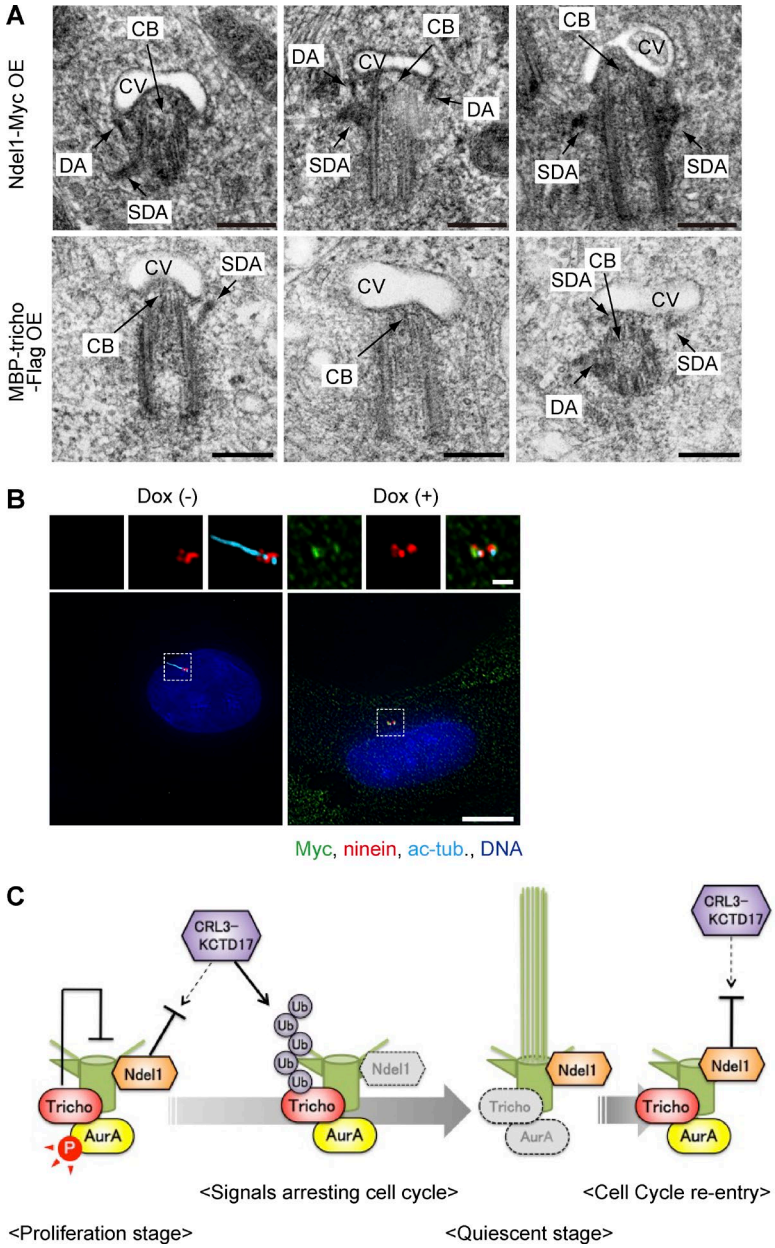

Figure 8. **The microstructure of mother centriole/basal body in cells expressing Ndel1-Myc or MBP-trichoplein-Flag under cultivation without serum.** (A and B) Each RPE1 cell line allowing inducible expression of Ndel1-Myc or MBP-trichoplein-Flag was cultured in the serum-free medium with 30 or 300 ng/ml Dox, respectively. 24 h after incubation, treated cells were subjected to TEM (A) or immunostaining (B). Micrographs show distinct mother centrioles and basal bodies (single sections). CB, ciliary bud; CV, ciliary vesicle; DA, distal appendage; SDA, subdistal appendage. Bars: (A) 200 nm; (B, main) 5 µm; (B, insets) 1 µm. (C) The cartoon shows our proposed model. P, phosphate; Ub, ubiquitin; Tricho, trichoplein; AurA, Aurora A.

also limits ciliary length during quiescence in Swiss 3T3 cells, further sustaining the observation in the kidney of newborn *NDEL1*$^{cko/cko}$ (Fig. 9, E and G).

Discussion

In the present study, we have discovered a novel function of Ndel1 in promoting cell cycle progression through the inhibition of ciliogenesis in proliferating cells (Figs. 1 and 4). This function likely requires Ndel1 associated with the subdistal appendage of the mother centriole (Fig. S3). During the course of ciliogenesis, Ndel1 is transiently decreased at the centrosome just before trichoplein degradation starts (Fig. 5). This transient Ndel1 degradation is required for axonemal MT extension during ciliogenesis (Figs. 6 and 8).

How does Ndel1 exert these functions? In the presence of serum, Ndel1 knockdown not only induces unscheduled primary cilia reassembly (Fig. 1) but also decreases mother-centriole–associated trichoplein (Fig. 7 E). The unscheduled cilia formation is restored by exogenous trichoplein induction (Fig. 7 B) or KCTD17 codepletion (a treatment suppressing trichoplein degradation at the mother centriole; Fig. 7, D and E). In serum-starved cells, Ndel1 induction increases mother-centriole–associated trichoplein and blocks primary cilia assembly (Fig. 6). Upon serum depletion, we observed only marginal differences in the morphology of mother centrioles and basal bodies among exogenous Ndel1 and trichoplein induction (Fig. 8 A) and KCTD17 knockdown (Kasahara et al., 2014). These observations led us to suggest the following model (Fig. 8 C). Ndel1 protects mother-centriole–associated trichoplein from CRL3^{KCTD17}-mediated degradation. The stabilized trichoplein binds Aurora A, which stimulates its autophosphorylation (Inoko et al., 2012). This elevation of the kinase activity destabilizes axonemal MTs, resulting in the deciliation at the cell cycle reentry (Pugacheva et al., 2007) or the

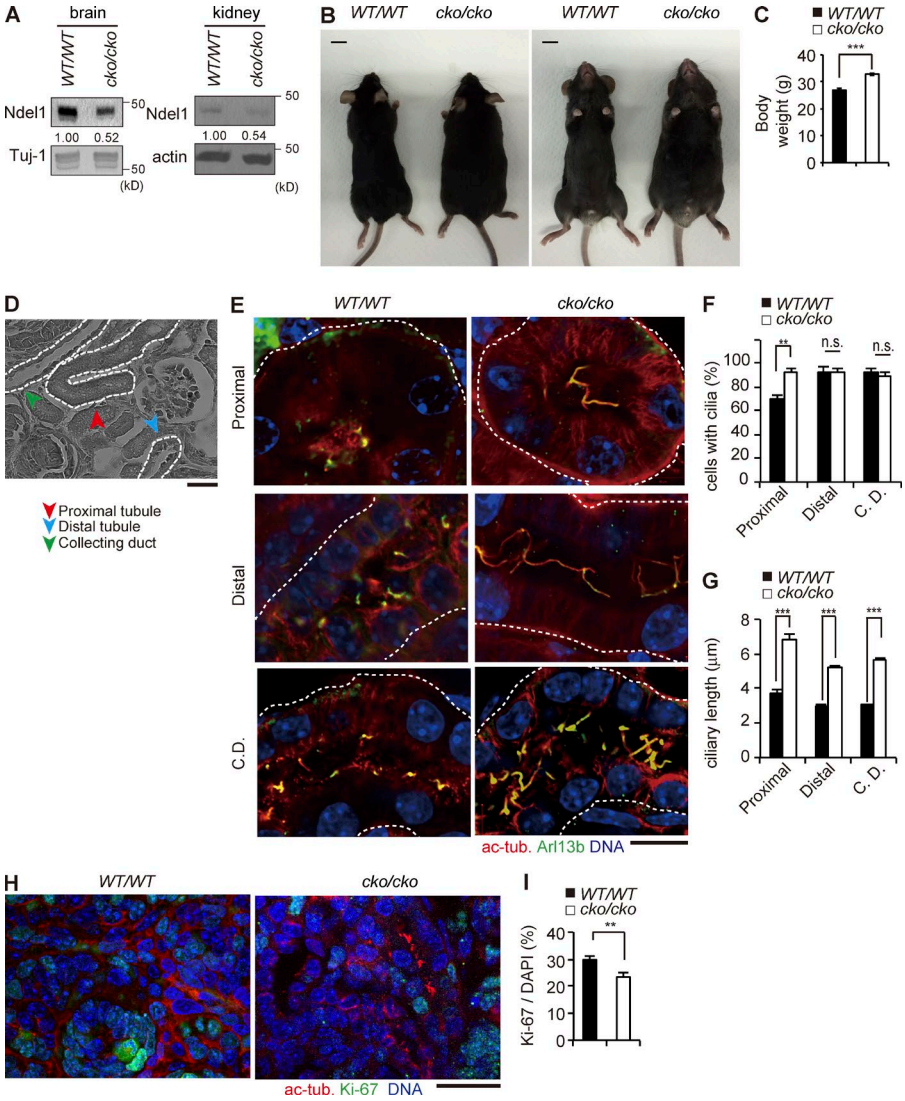

Figure 9. **Ndel1 negatively regulates primary cilia assembly in the kidney of newborn mice.** (A) Total protein was extracted from brains or kidneys of *NDEL1*$^{WT/WT}$ or *NDEL1*$^{cko/cko}$ mice at 3 mo of age and subjected to immunoblotting. Relative amounts of Ndel1 were quantified using densitometry, normalized to the content of actin. (B) A male *NDEL1*$^{WT/WT}$ (left) or *NDEL1*$^{cko/cko}$ (right) mouse at 3 mo of age. (C) Mean body weight of *NDEL1*$^{WT/WT}$ or *NDEL1*$^{cko/cko}$ mice at 4 mo of age (n = 5 mice each). (D) hematoxylin and eosin staining of a kidney from a mouse. A red, blue, or green arrowhead indicates proximal or distal tubule or collecting duct (C.D.), respectively. (E) Kidney from the newborn *NDEL1*$^{WT/WT}$ or *NDEL1*$^{cko/cko}$ mice was stained with anti–acetylated tubulin (red), anti-Arl13b (green), and DAPI (DNA; blue). White dashed line indicates the border of each renal tubule/duct. (F and G) The percentage of ciliated cells (F) and mean length of primary cilia (G) in kidney of newborn mice are shown in the graphs. For calculation, we used >50 cells from $n \geq 5$ (F) or 20 (G) mice per each category. (H) Kidney sections from the indicated newborn mice were stained with anti–acetylated tubulin (red) anti-Ki-67 (green) and DAPI (blue). (I) We quantified the percentage of Ki-67–positive cells, using >800 cells from three mice. Bars: (B) 1 cm; (E) 10 μm; (D) 20 μm; (H) 25 μm.

inhibition of unscheduled ciliary assembly (Inoko et al., 2012; Kasahara et al., 2014).

Judged by our pull-down (Fig. S5, A and B) and in vitro binding (Fig. S5, C and D) assays, Ndel1 is unlikely to directly bind trichoplein or the CRL3^{KCTD17} complex. Our in vitro analyses also revealed that Ndel1 might not directly inhibit CRL3^{KCTD17}-mediated trichoplein ubiquitination (Fig. S5 E). These observations raise the question of how Ndel1 inhibits CRL3^{KCTD17}-mediated trichoplein degradation. We consider the following two possibilities. (1) Because Ndel1 functions as a scaffold protein (Yamada et al., 2010; Chansard et al., 2011a; Bradshaw et al., 2013), its binding partners may directly suppress CRL3^{KCTD17}-mediated trichoplein degradation through the interaction with trichoplein or CRL3^{KCTD17} complex (also see next chapter). (2) Ndel1 may function as a gate equipped in the mother centriole. When Ndel1 exists in subdistal appendages, this gate is closed and the CRL3^{KCTD17} complex can therefore scarcely enter mother centriole. When Ndel1 is removed from the appendages (e.g., by Ndel1 depletion or in response to serum depletion), the gate is open and then CRL3^{KCTD17} complex is able to attack mother-centriole–associated trichoplein.

Accumulating evidence has revealed that Ndel1 and NDE1 share some common functions but also exert unique functions (Bradshaw et al., 2013). Two proteins are also known to modulate dynein activity (Yamada et al., 2010; Chansard et al., 2011a; Bradshaw et al., 2013). These observations raise the question of whether Ndel1 controls ciliary dynamics coordinately with dynein and dynein-associated proteins. With regard to ciliary absorption at cell cycle reentry, knockdown of NDE1 (Fig. 2, A and B; Kim et al., 2011) or dynein (Fig. 3, G, J, and M) produces phenotypes similar to Ndel1 knockdown. However, NDE1 (Fig. 2 C; Kim et al., 2011) or dynein (Palmer et al., 2011) also limits ciliary length in quiescent RPE1 cells, which raises the possibility that abnormally longer cilia may affect ciliary resorption processes at cell cycle reentry. Meanwhile, Ndel1 depletion has no effect on ciliary length in quiescent RPE1 cells (Fig. 2 C). Furthermore, unlike Ndel1, NDE1 (Fig. 1) or dynein (Fig. 3, E, F, H, I, K, and L) only marginally contribute the process to suppress ciliogenesis in proliferating RPE1 cells. Together with the in vitro binding and ubiquitination analyses (Fig. S5), these observations increase the possibility that NDE1 and/or dynein may control ciliary dynamics in a way different from Ndel1. In contrast, ciliary phenotypes of Lis1 depletion resemble those of Ndel1 depletion (Fig. 3, A–D). Thus, Lis1 may be one of likely candidates to transduce Ndel1 signaling. However, we cannot rule out the possibility

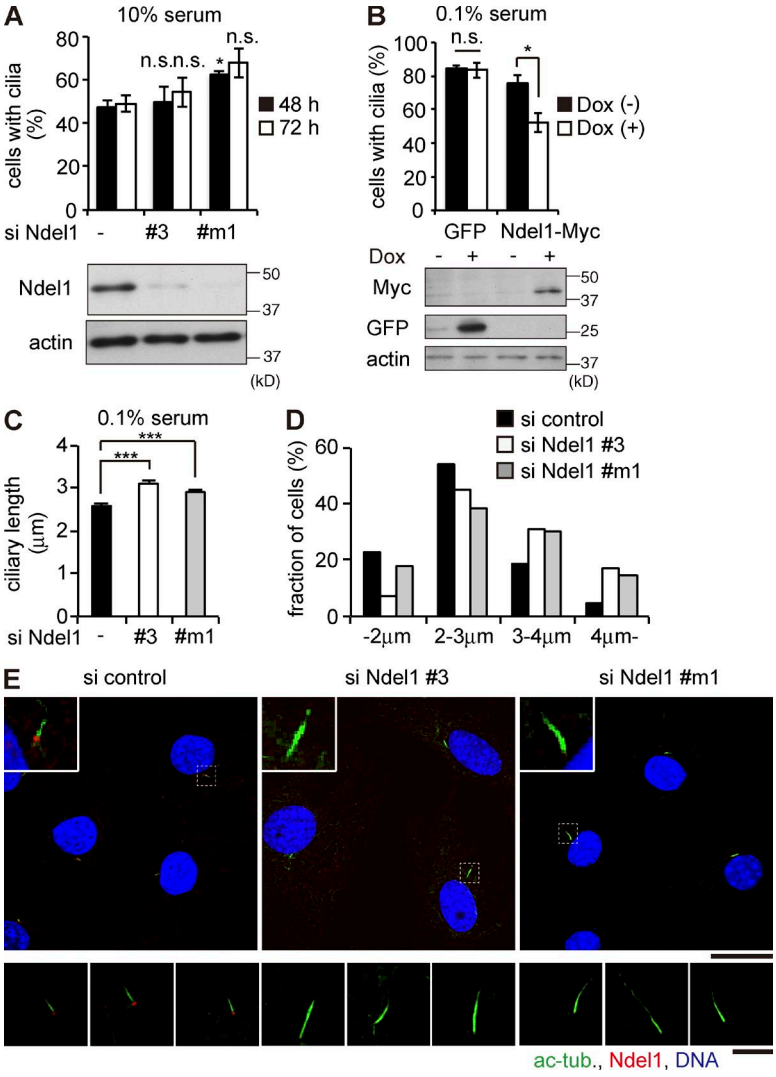

Figure 10. **Ndel1 negatively controls ciliary length in Swiss 3T3 cells.** (A) Swiss 3T3 cells were treated with each Ndel1-specific siRNA (target sequence 3 or m1) or control siRNA for 48 or 72 h. Cell lysates were immunoblotting with anti-Ndel1 and anti-actin. (B) Tet-On Swiss 3T3 cell line expressing inducible GFP or Ndel1-Myc was incubated with (+) or without (–) 30 ng/ml Dox in the growing medium for 24 h and then in the medium containing 0.1% serum for 24 h. Cell lysates were immunoblotting with anti-Myc, anti-GFP, and anti-actin. The data are shown as mean ± SEM from three independent experiments (n > 100 each; A, B, and C–E) Swiss 3T3 cells were treated with the indicated siRNA. 24 h after transfection, the medium was changed to new medium containing 0.1% serum. Then, the cells were incubated for additional 48 h. Averaged (C) and distribution (D) of ciliary length are shown in the graphs. Ciliary length from 40 cells was measured for each experiment (means ± SEM; n = 3 independent experiments). The treated cells were stained with anti–acetylated tubulin (ac-tub.; green), anti-Ndel1 (red), and DAPI (blue; E). *, P < 0.05; ***, P < 0.001; n.s., not significant; two-tailed unpaired t test. Bars: (E, bottom) 5 μm; (E, top) 10 μm.

that Lis1 and Ndel1 may regulate ciliary dynamics in different ways, because these are a few apparent differences in their knockdown phenotypes (e.g., nucleus–centrosome coupling or ciliary length in quiescent RPE1 cells).

Both Ndel1 protein level and centrosome-associated Ndel1 are transiently decreased but finally recovered after serum starvation (Fig. 5). Because primary cilia are lengthened by reduced expression of Ndel1 in newborn mouse kidney (Fig. 9, E and G) or serum-starved Swiss 3T3 cells (Fig. 10, C–E), Ndel1 also limits ciliary length during quiescent state. Thus, after the construction of primary cilia, Ndel1 returns to the basal body and may adjust proper ciliary length, a process required for the maintenance of primary cilia. These observations also raise a new question of why Ndel1 knockdown did not affect ciliary length in quiescent RPE1 cells (Fig. 2 C). One possible explanation is the existence of NDE1, which reportedly limited ciliary length during ciliogenesis (Kim et al., 2011). With regard to ciliary length control, NDE1 may compensate for reduced Ndel1 expression in some types of cells, such as RPE1 cells. Because the recovery of Ndel1 at the centrosome unlikely affects the behavior of trichoplein after serum starvation (Fig. 5, A–D), Ndel1 may control other targets to limit ciliary length. In this regard, NDE1 negatively regulates ciliary length via the interaction with a dynein light-chain protein, LC8 (Kim et al., 2011). In addition, dynein complexes share similar function in RPE1 cells (Fig. 3, G, J, and M; Palmer et al., 2011). Therefore, like NDE1, Ndel1 may also limit ciliary length by modulating dynein activity.

The present study documents novel functions of Ndel1 as a negative regulator of ciliary assembly and paves the way for future studies evaluating the importance of ciliary dynamics in development and tissue homeostasis.

Materials and methods

Antibodies

Commercial antibodies and their dilution were as follows: mouse anti–acetylated α-tubulin diluted at 1:200 (clone 6-11B-1; Sigma-Aldrich), anti–α-tubulin diluted at 1:100 (clone DM 1A; Sigma-Aldrich), anti–cyclin A antibody diluted at 1:100 for immunofluorescence and at 1:1,000 for immunoblotting (cyclin A clone 25; BD Biosciences), anti–centrin 2 diluted at 1:100 (clone 20H5; Merck Millipore), anti-dynein intermediate chain diluted at 1: 1,000 (clone 74.1; Merck Millipore), anti-Flag diluted at 1:10,000 (clone M2, Sigma-Aldrich), anti-Myc diluted at 1:1,000 (clone 9B11; Cell Signaling Technology; or clone 4A6; Merck Millipore), rabbit anti–phospho–Aurora A (Thr288) antibody diluted at 1:1,000 (clone C39D8; Cell Signaling Technology),

anti-CEP164 antibody diluted at 1:100 (Sigma-Aldrich), anti-DYNC1H1 antibody diluted at 1:1,000 (Proteintech Group), anti-DYNC1I2 antibody diluted at 1:1,000 (Proteintech Group), anti-DYNLT1 (Tctex-1) diluted at 1:1,000 (Proteintech Group), anti-IFT20 antibody diluted at 1:1,000 (Proteintech Group), anti-Lis1 antibody diluted at 1:1,000 (Santa Cruz Biotechnology), anti-NDE1 antibody diluted at 1:3,000 (Proteintech Group), anti-Odf2 antibody diluted at 1:100 for immunofluorescence and at 1:500 for immunoblotting (Sigma-Aldrich), anti-ninein diluted at 1:100 for immunofluorescence (BioLegend) and at 1:1,000 for immunoblotting (a gift from A. Kikuchi, Osaka University, Osaka, Japan; Fumoto et al., 2006), and goat anti-actin antibody diluted at 1:1,000 (Santa Cruz Biotechnology). The following rabbit polyclonal antibodies were produced as described previously (Sasaki et al., 2000; Nishizawa et al., 2005; Ibi et al., 2011; Kasahara et al., 2014): anti-KCTD17 diluted at 1:20,000, anti-Ndel1 diluted at 1:3,000–1:5,000, and anti-trichoplein diluted at 1:200 for immunofluorescence and at 1: 2,000 for immunoblotting. Fluorescent secondary antibodies and Zenon antibody labeling kits were obtained from Molecular Probes and Life Technologies.

Cell culture

hTERT-immortalized human retinal pigment epithelial (RPE1) cells were cultured in DMEM and F12 nutrient mix (1:1) supplemented with 10% FBS. HeLa and Swiss 3T3 cells were cultured in DMEM supplemented with 10% FBS. MG132, Lactacystin, and ALLN were purchased from Merck. Epoxomicin was obtained from the Peptide Institute.

Establishment of Tet-On RPE1 or Swiss 3T3 cell lines

Tet-On RPE1 or Swiss 3T3 cell lines that expressed GFP, MBP-trichoplein-Flag, NDE1-Myc, or RNAi-resistant Ndel1-Myc (isoform A, B, and Δ256–291) were established as described previously (Ibi et al., 2011; Li et al., 2011). For induction, Tet-On RPE1 or Swiss 3T3 cells were treated with 3–300 ng/ml Dox (Sigma-Aldrich).

siRNAs

Transfection of siRNA duplexes was performed with Lipofectamine RNAiMAX reagent according to the manufacturer's protocol (Life Technologies); each duplex for Odf2, IFT20, or others was used at final concentration of 20, 50, or 10 nM, respectively. The double-stranded RNAs were purchased from Qiagen or Ambion and Life Technologies. Target nucleotide sequences are shown in Table S2. Negative control 2 siRNA (Silencer Select; Life Technologies) was used as a negative control.

Immunofluorescence microscopy

Immunofluorescence microscopy was performed using confocal microscopy (LSM510 META; Carl Zeiss) equipped with a microscope (Axiovert 200M; Carl Zeiss), a plan Apochromat 100×/1.4 NA oil-immersion lens, and LSM image browser software (Carl Zeiss) or a DeltaVision system (Applied Precision) equipped with a microscope (IX70; Olympus), a Plan Apochromat 100×/1.4 NA oil-immersion lens, a cooled charge-coupled device camera, and softWoRx software (Applied Precision) as described previously (Inoko et al., 2012). RPE1, HeLa, and Swiss 3T3 cells were grown on coverslips (Iwaki Glass) and fixed with methanol or formaldehyde as described previously (Sugimoto et al., 2008). For immunostaining with anti-trichoplein, cells were fixed with −20°C methanol for 10 min after 0.01% saponin in PBS at room temperature for 15 min. For detection of primary cilia, cells were placed on ice for 30 min before fixation and stained with anti–acetylated tubulin antibody (Inoko et al., 2012). BrdU incorporation was evaluated using the DNA Replication Assay kit (Merck Millipore). Quantification of fluorescence intensity was performed using ImageJ 1.47v Software (National Institutes of Health). Ciliary length of cultured cells was measured using LSM image browser software. Immunofluorescence images of mouse kidneys were acquired using confocal microscopy (LSM700; Carl Zeiss) equipped with a plan Apochromat 100×/1.4 NA oil-immersion lens and Zen software (Carl Zeiss). *NDEL1*$^{WT/WT}$ and *NDEL1*$^{cko/cko}$ newborn mouse kidneys were fixed with 4% paraformaldehyde overnight and embedded in Optimal Cutting Temperature compound (Sakura Finetek) after 30% sucrose infiltration and processed for immunofluorescence. Kidney sections were permeabilized with 0.3% Triton X-100. Reconstructed images were used to determine cilium length and rates of cilia formation as follows. To calculate cilia length, points corresponding to the ciliary base and tip form a right triangle with a third point corresponding to a projection of tip on the x, y plane. In this triangle, the hypotenuse is the cilia length. For rates of cilia formation, objects (cells and cilia) were defined in the 3D images and numbers of object obtained for each. All images were taken at room temperature. Figures were generated using Photoshop Elements 11 and Illustrator CS6 (Adobe).

Protein purification

Cul3-3xFlag and Rbx1-GFP were coexpressed in HEK293T cells using Lipofectamine 2000. 1 d after transfection, cells were lysed in cell lysis buffer (20 mM Tris-HCl, pH 7.5, 150 mM NaCl, 2 mM β-glycerophosphate, 50 mM NaF, 1 mM Na_3VO_4, 2.5 mM sodium pyrophosphate, 2 mM EDTA, 1 mM EGTA, and 1% Triton X-100) containing protease inhibitor cocktail (Nacalai Tesque). Cul3-3xFlag immunocomplexes immobilized on anti–DYKDDDDK-tag antibody beads (Wako Laboratory Chemicals) were washed three times with cell lysis buffer and twice with TBS (50 mM Tris-HCl, pH 7.4, 150 mM NaCl) and then eluted with 100 µg/ml 3xFlag peptide (Sigma-Aldrich) dissolved in PBS containing 0.1% Tween 20 (PBST). For protein purification from bacteria, Ndel1 or NDE1 with an N-terminal His-tag and C-terminal Myc-tag was expressed in BL21-CodonPlus (DE3)-RIPL (Agilent Technologies) and then purified through nickel-affinity chromatography according to manufacturer's protocol (Qiagen). GST-tagged KCTD17 and MBP-trichoplein were expressed in DH5α strain (Invitrogen) and BL21 CodonPlus RP stain (Agilent Technologies), respectively. Each protein was purified through the affinity chromatography with glutathione-Sepharose 4B (GE Healthcare) or amylose resin (New England Biolabs).

Pull-down assays

Bacterially purified GST-KCTD17 (20 µg) or His-Ndel1/NDE1-myc (10 µg) was incubated with RPE1 cell lysates for 3 h at 4°C and then affinity purified with glutathione-sepharose 4B beads (GE Healthcare) or anti–c-Myc (MC045) agarose conjugate beads (Nacalai Tesque), respectively. After washing with cell lysis buffer three times, the beads were subjected to immunoblotting.

In vitro binding assay

MBP-trichoplein (1.0 µg), Cul3-3xFlag immunocomplex (0.3 µg), and GST-KCTD17 (1.0 µg) were incubated in cell lysis buffer in the presence of His-Ndel1-myc (1.0 µg) or His-NDE1-myc (1.0 µg) for 3 h at 4°C. The mixtures were subjected to immunoprecipitation using anti-GST (Cell Signaling Technology) or anti-Myc (MC045).

In vitro ubiquitynation assay

His-ubiquitin (12 µg; LifeSensors), MBP-trichoplein (1.0 µg), Cul3-3xFlag immunocomplex (0.1 µg), GST-KCTD17 (1.0 µg), His-Ube1 (0.4 µg; ENZO Life Sciences), and His-UbcH5a (0.5 µg; Enzo Life Sciences) were incubated in 30-µl reaction mixture (50 mM Tris-HCl, pH 7.5, 5 mM $MgCl_2$, 2 mM NaF, 2 mM ATP, and 0.6 mM DTT) in

the presence or absence of His-Ndel1/NDE1-Myc (1.0 µg) at 37°C for 1 h. The reaction was subjected to immunoprecipitation using anti-trichoplein before immunoblotting with anti-ubiquitin.

Other methods

Immunoblotting (Kasahara et al., 2014), FACS analysis (Inoko et al., 2012), TEM observation (Inoko et al., 2012), and the MT regrowth assay (Ibi et al., 2011) were performed as described previously.

Online supplemental material

Fig. S1 shows localization of Ndel1 at the centrosome. Fig. S2 demonstrates relationship between Ndel1 and Odf2 or ninein. Fig. S3 shows that centrosomal targeting domain of Ndel1 is necessary to inhibit unscheduled primary cilia assembly in proliferating cells. Fig. S4 demonstrates electron microscopic analysis of a basal body/mother centriole in serum-starved, Ndel1-overexpressing cells. Fig. S5 shows that Ndel1 neither interacts with trichoplein or Cul3-KCTD17 nor affects ubiqutination of trichoplein by Cul3-KCTD17 in vitro. Table S1 lists THPD-containing proteins for siRNA screening. Table S2 lists siRNA sequences used in this study. Online supplemental material is available at http://www.jcb.org/cgi/content/full/jcb.201507046/DC1. Additional data are available in the JCB DataViewer at http://dx.doi.org/10.1083/jcb.201507046.dv.

Acknowledgments

We thank Y. Hayashi, N. Tanigawa, K. Kobori, and E. Kawamoto for technical assistance; H. Tanaka for the FACS analysis; M. Aoki for helpful discussion, and A. Kikuchi for the gift of rabbit polyclonal anti-ninein antibody. We are grateful to R.A. Quinlan and T. Magin for helpful discussion and critical comments on the manuscript.

This work was supported in part by Grants-in-Aid for Scientific Research from the Japan Society for the Promotion of Science and from the Ministry of Education, Culture, Sports, Science, and Technology of Japan; by research grants from the Takeda Science Foundation, the Astellas Foundation for Research on Metabolic Disorders, and the Princess Takamatsu Cancer Research Fund; and by the Uehara Memorial Foundation.

The authors declare no competing financial interests.

Submitted: 13 July 2015
Accepted: 12 January 2016

References

Anderson, C.T., A.B. Castillo, S.A. Brugmann, J.A. Helms, C.R. Jacobs, and T. Stearns. 2008. Primary cilia: cellular sensors for the skeleton. *Anat. Rec. (Hoboken).* 291:1074–1078. http://dx.doi.org/10.1002/ar.20754

Bradshaw, N.J., D.C. Soares, B.C. Carlyle, F. Ogawa, H. Davidson-Smith, S. Christie, S. Mackie, P.A. Thomson, D.J. Porteous, and J.K. Millar. 2011. PKA phosphorylation of NDE1 is DISC1/PDE4 dependent and modulates its interaction with LIS1 and NDEL1. *J. Neurosci.* 31:9043–9054. http://dx.doi.org/10.1523/JNEUROSCI.5410-10.2011

Bradshaw, N.J., W. Hennah, and D.C. Soares. 2013. NDE1 and NDEL1: twin neurodevelopmental proteins with similar 'nature' but different 'nurture'. *Biomol. Concepts.* 4:447–464. http://dx.doi.org/10.1515/bmc-2013-0023

Chansard, M., J.H. Hong, Y.U. Park, S.K. Park, and M.D. Nguyen. 2011a. Ndel1, Nudel (Noodle): flexible in the cell? *Cytoskeleton (Hoboken).* 68:540–554. http://dx.doi.org/10.1002/cm.20532

Chansard, M., J. Wang, H.C. Tran, G. Neumayer, S.Y. Shim, Y.U. Park, C. Belzil, H.T. Le, S.K. Park, and M.D. Nguyen. 2011b. The cytoskeletal protein Ndel1 regulates dynamin 2 GTPase activity. *PLoS One.* 6:e14583. http://dx.doi.org/10.1371/journal.pone.0014583

Dammermann, A., and A. Merdes. 2002. Assembly of centrosomal proteins and microtubule organization depends on PCM-1. *J. Cell Biol.* 159:255–266. http://dx.doi.org/10.1083/jcb.200204023

Delgehyr, N., J. Sillibourne, and M. Bornens. 2005. Microtubule nucleation and anchoring at the centrosome are independent processes linked by ninein function. *J. Cell Sci.* 118:1565–1575. http://dx.doi.org/10.1242/jcs.02302

Follit, J.A., R.A. Tuft, K.E. Fogarty, and G.J. Pazour. 2006. The intraflagellar transport protein IFT20 is associated with the Golgi complex and is required for cilia assembly. *Mol. Biol. Cell.* 17:3781–3792. http://dx.doi.org/10.1091/mbc.E06-02-0133

Fumoto, K., C.C. Hoogenraad, and A. Kikuchi. 2006. GSK-3beta-regulated interaction of BICD with dynein is involved in microtubule anchorage at centrosome. *EMBO J.* 25:5670–5682. http://dx.doi.org/10.1038/sj.emboj.7601459

Gerdes, J.M., E.E. Davis, and N. Katsanis. 2009. The vertebrate primary cilium in development, homeostasis, and disease. *Cell.* 137:32–45. http://dx.doi.org/10.1016/j.cell.2009.03.023

Goetz, S.C., and K.V. Anderson. 2010. The primary cilium: a signalling centre during vertebrate development. *Nat. Rev. Genet.* 11:331–344. http://dx.doi.org/10.1038/nrg2774

Goto, H., A. Inoko, and M. Inagaki. 2013. Cell cycle progression by the repression of primary cilia formation in proliferating cells. *Cell. Mol. Life Sci.* 70:3893–3905. http://dx.doi.org/10.1007/s00018-013-1302-8

Graser, S., Y.D. Stierhof, S.B. Lavoie, O.S. Gassner, S. Lamla, M. Le Clech, and E.A. Nigg. 2007. Cep164, a novel centriole appendage protein required for primary cilium formation. *J. Cell Biol.* 179:321–330. http://dx.doi.org/10.1083/jcb.200707181

Guo, J., Z. Yang, W. Song, Q. Chen, F. Wang, Q. Zhang, and X. Zhu. 2006. Nudel contributes to microtubule anchoring at the mother centriole and is involved in both dynein-dependent and -independent centrosomal protein assembly. *Mol. Biol. Cell.* 17:680–689. http://dx.doi.org/10.1091/mbc.E05-04-0360

Ibi, M., P. Zou, A. Inoko, T. Shiromizu, M. Matsuyama, Y. Hayashi, M. Enomoto, D. Mori, S. Hirotsune, T. Kiyono, et al. 2011. Trichoplein controls microtubule anchoring at the centrosome by binding to Odf2 and ninein. *J. Cell Sci.* 124:857–864. http://dx.doi.org/10.1242/jcs.075705

Inoko, A., M. Matsuyama, H. Goto, Y. Ohmuro-Matsuyama, Y. Hayashi, M. Enomoto, M. Ibi, T. Urano, S. Yonemura, T. Kiyono, et al. 2012. Trichoplein and Aurora A block aberrant primary cilia assembly in proliferating cells. *J. Cell Biol.* 197:391–405. http://dx.doi.org/10.1083/jcb.201106101

Ishikawa, H., and W.F. Marshall. 2011. Ciliogenesis: building the cell's antenna. *Nat. Rev. Mol. Cell Biol.* 12:222–234. http://dx.doi.org/10.1038/nrm3085

Ishikawa, H., A. Kubo, S. Tsukita, and S. Tsukita. 2005. Odf2-deficient mother centrioles lack distal/subdistal appendages and the ability to generate primary cilia. *Nat. Cell Biol.* 7:517–524. http://dx.doi.org/10.1038/ncb1251

Kasahara, K., Y. Kawakami, T. Kiyono, S. Yonemura, Y. Kawamura, S. Era, F. Matsuzaki, N. Goshima, and M. Inagaki. 2014. Ubiquitin-proteasome system controls ciliogenesis at the initial step of axoneme extension. *Nat. Commun.* 5:5081. http://dx.doi.org/10.1038/ncomms6081

Kim, S., and L. Tsiokas. 2011. Cilia and cell cycle re-entry: more than a coincidence. *Cell Cycle.* 10:2683–2690. http://dx.doi.org/10.4161/cc.10.16.17009

Kim, J.Y., X. Duan, C.Y. Liu, M.H. Jang, J.U. Guo, N. Pow-anpongkul, E. Kang, H. Song, and G.L. Ming. 2009. DISC1 regulates new neuron development in the adult brain via modulation of AKT-mTOR signaling through KIAA1212. *Neuron.* 63:761–773. http://dx.doi.org/10.1016/j.neuron.2009.08.008

Kim, S., N.A. Zaghloul, E. Bubenshchikova, E.C. Oh, S. Rankin, N. Katsanis, T. Obara, and L. Tsiokas. 2011. Nde1-mediated inhibition of ciliogenesis affects cell cycle re-entry. *Nat. Cell Biol.* 13:351–360. http://dx.doi.org/10.1038/ncb2183

Kinzel, D., K. Boldt, E.E. Davis, I. Burtscher, D. Trümbach, B. Diplas, T. Attié-Bitach, W. Wurst, N. Katsanis, M. Ueffing, and H. Lickert. 2010. Pitchfork regulates primary cilia disassembly and left-right asymmetry. *Dev. Cell.* 19:66–77. http://dx.doi.org/10.1016/j.devcel.2010.06.005

Lange, B.M., and K. Gull. 1995. A molecular marker for centriole maturation in the mammalian cell cycle. *J. Cell Biol.* 130:919–927. http://dx.doi.org/10.1083/jcb.130.4.919

Laoukili, J., E. Perret, S. Middendorp, O. Houcine, C. Guennou, F. Marano, M. Bornens, and F. Tournier. 2000. Differential expression and cellular distribution of centrin isoforms during human ciliated cell differentiation in vitro. *J. Cell Sci.* 113:1355–1364.

Li, A., M. Saito, J.Z. Chuang, Y.Y. Tseng, C. Dedesma, K. Tomizawa, T. Kaitsuka, and C.H. Sung. 2011. Ciliary transition zone activation of phosphorylated Tctex-1 controls ciliary resorption, S-phase entry and fate of neural progenitors. *Nat. Cell Biol.* 13:402–411. http://dx.doi.org/10.1038/ncb2218

Li, P., H. Goto, K. Kasahara, M. Matsuyama, Z. Wang, Y. Yatabe, T. Kiyono, and M. Inagaki. 2012. P90 RSK arranges Chk1 in the nucleus for monitoring of genomic integrity during cell proliferation. *Mol. Biol. Cell.* 23:1582–1592. http://dx.doi.org/10.1091/mbc.E11-10-0883

Li, Y., N.T. Klena, G.C. Gabriel, X. Liu, A.J. Kim, K. Lemke, Y. Chen, B. Chatterjee, W. Devine, R.R. Damerla, et al. 2015. Global genetic analysis in mice unveils central role for cilia in congenital heart disease. *Nature.* 521:520–524. http://dx.doi.org/10.1038/nature14269

Liang, Y., W. Yu, Y. Li, Z. Yang, X. Yan, Q. Huang, and X. Zhu. 2004. Nudel functions in membrane traffic mainly through association with Lis1 and cytoplasmic dynein. *J. Cell Biol.* 164:557–566. http://dx.doi.org/10.1083/jcb.200308058

Mogensen, M.M., A. Malik, M. Piel, V. Bouckson-Castaing, and M. Bornens. 2000. Microtubule minus-end anchorage at centrosomal and non-centrosomal sites: the role of ninein. *J. Cell Sci.* 113:3013–3023.

Molla-Herman, A., R. Ghossoub, T. Blisnick, A. Meunier, C. Serres, F. Silbermann, C. Emmerson, K. Romeo, P. Bourdoncle, A. Schmitt, et al. 2010. The ciliary pocket: an endocytic membrane domain at the base of primary and motile cilia. *J. Cell Sci.* 123:1785–1795. http://dx.doi.org/10.1242/jcs.059519

Mori, D., M. Yamada, Y. Mimori-Kiyosue, Y. Shirai, A. Suzuki, S. Ohno, H. Saya, A. Wynshaw-Boris, and S. Hirotsune. 2009. An essential role of the aPKC-Aurora A-NDEL1 pathway in neurite elongation by modulation of microtubule dynamics. *Nat. Cell Biol.* 11:1057–1068. http://dx.doi.org/10.1038/ncb1919

Murray, A.W. 2004. Recycling the cell cycle: cyclins revisited. *Cell.* 116:221–234. http://dx.doi.org/10.1016/S0092-8674(03)01080-8

Nakagawa, Y., Y. Yamane, T. Okanoue, S. Tsukita, and S. Tsukita. 2001. Outer dense fiber 2 is a widespread centrosome scaffold component preferentially associated with mother centrioles: its identification from isolated centrosomes. *Mol. Biol. Cell.* 12:1687–1697. http://dx.doi.org/10.1091/mbc.12.6.1687

Niethammer, M., D.S. Smith, R. Ayala, J. Peng, J. Ko, M.S. Lee, M. Morabito, and L.H. Tsai. 2000. NUDEL is a novel Cdk5 substrate that associates with LIS1 and cytoplasmic dynein. *Neuron.* 28:697–711. http://dx.doi.org/10.1016/S0896-6273(00)00147-1

Nigg, E.A., and J.W. Raff. 2009. Centrioles, centrosomes, and cilia in health and disease. *Cell.* 139:663–678. http://dx.doi.org/10.1016/j.cell.2009.10.036

Nishizawa, M., I. Izawa, A. Inoko, Y. Hayashi, K. Nagata, T. Yokoyama, J. Usukura, and M. Inagaki. 2005. Identification of trichoplein, a novel keratin filament-binding protein. *J. Cell Sci.* 118:1081–1090. http://dx.doi.org/10.1242/jcs.01667

Ou, Y.Y., G.J. Mack, M. Zhang, and J.B. Rattner. 2002. CEP110 and ninein are located in a specific domain of the centrosome associated with centrosome maturation. *J. Cell Sci.* 115:1825–1835.

Palmer, K.J., L. MacCarthy-Morrogh, N. Smyllie, and D.J. Stephens. 2011. A role for Tctex-1 (DYNLT1) in controlling primary cilium length. *Eur. J. Cell Biol.* 90:865–871. http://dx.doi.org/10.1016/j.ejcb.2011.05.003

Paoletti, A., M. Moudjou, M. Paintrand, J.L. Salisbury, and M. Bornens. 1996. Most of centrin in animal cells is not centrosome-associated and centrosomal centrin is confined to the distal lumen of centrioles. *J. Cell Sci.* 109:3089–3102.

Plotnikova, O.V., A.S. Nikonova, Y.V. Loskutov, P.Y. Kozyulina, E.N. Pugacheva, and E.A. Golemis. 2012. Calmodulin activation of Aurora-A kinase (AURKA) is required during ciliary disassembly and in mitosis. *Mol. Biol. Cell.* 23:2658–2670. http://dx.doi.org/10.1091/mbc.E11-12-1056

Pugacheva, E.N., S.A. Jablonski, T.R. Hartman, E.P. Henske, and E.A. Golemis. 2007. HEF1-dependent Aurora A activation induces disassembly of the primary cilium. *Cell.* 129:1351–1363. http://dx.doi.org/10.1016/j.cell.2007.04.035

Quarmby, L.M., and J.D. Parker. 2005. Cilia and the cell cycle? *J. Cell Biol.* 169:707–710. http://dx.doi.org/10.1083/jcb.200503053

Sasaki, S., A. Shionoya, M. Ishida, M.J. Gambello, J. Yingling, A. Wynshaw-Boris, and S. Hirotsune. 2000. A LIS1/NUDEL/cytoplasmic dynein heavy chain complex in the developing and adult nervous system. *Neuron.* 28:681–696. http://dx.doi.org/10.1016/S0896-6273(00)00146-X

Sasaki, S., D. Mori, K. Toyo-oka, A. Chen, L. Garrett-Beal, M. Muramatsu, S. Miyagawa, N. Hiraiwa, A. Yoshiki, A. Wynshaw-Boris, and S. Hirotsune. 2005. Complete loss of Ndel1 results in neuronal migration defects and early embryonic lethality. *Mol. Cell. Biol.* 25:7812–7827. http://dx.doi.org/10.1128/MCB.25.17.7812-7827.2005

Seeley, E.S., and M.V. Nachury. 2010. The perennial organelle: assembly and disassembly of the primary cilium. *J. Cell Sci.* 123:511–518. http://dx.doi.org/10.1242/jcs.061093

Singla, V., and J.F. Reiter. 2006. The primary cilium as the cell's antenna: signaling at a sensory organelle. *Science.* 313:629–633. http://dx.doi.org/10.1126/science.1124534

Sorokin, S.P. 1968. Reconstructions of centriole formation and ciliogenesis in mammalian lungs. *J. Cell Sci.* 3:207–230.

Sugimoto, M., A. Inoko, T. Shiromizu, M. Nakayama, P. Zou, S. Yonemura, Y. Hayashi, I. Izawa, M. Sasoh, Y. Uji, et al. 2008. The keratin-binding protein Albatross regulates polarization of epithelial cells. *J. Cell Biol.* 183:19–28. http://dx.doi.org/10.1083/jcb.200803133

Tanaka, T., F.F. Serneo, C. Higgins, M.J. Gambello, A. Wynshaw-Boris, and J.G. Gleeson. 2004. Lis1 and doublecortin function with dynein to mediate coupling of the nucleus to the centrosome in neuronal migration. *J. Cell Biol.* 165:709–721. http://dx.doi.org/10.1083/jcb.200309025

Tateishi, K., Y. Yamazaki, T. Nishida, S. Watanabe, K. Kunimoto, H. Ishikawa, and S. Tsukita. 2013. Two appendages homologous between basal bodies and centrioles are formed using distinct Odf2 domains. *J. Cell Biol.* 203:417–425. http://dx.doi.org/10.1083/jcb.201303071

Vergnolle, M.A., and S.S. Taylor. 2007. Cenp-F links kinetochores to Ndel1/Nde1/Lis1/dynein microtubule motor complexes. *Curr. Biol.* 17:1173–1179. http://dx.doi.org/10.1016/j.cub.2007.05.077

Yamada, M., S. Toba, Y. Yoshida, K. Haratani, D. Mori, Y. Yano, Y. Mimori-Kiyosue, T. Nakamura, K. Itoh, S. Fushiki, et al. 2008. LIS1 and NDEL1 coordinate the plus-end-directed transport of cytoplasmic dynein. *EMBO J.* 27:2471–2483. http://dx.doi.org/10.1038/emboj.2008.182

Yamada, M., S. Hirotsune, and A. Wynshaw-Boris. 2010. The essential role of LIS1, NDEL1 and Aurora-A in polarity formation and microtubule organization during neurogensis. *Cell Adhes. Migr.* 4:180–184. http://dx.doi.org/10.4161/cam.4.2.10715

Zyłkiewicz, E., M. Kijańska, W.C. Choi, U. Derewenda, Z.S. Derewenda, and P.T. Stukenberg. 2011. The N-terminal coiled-coil of Ndel1 is a regulated scaffold that recruits LIS1 to dynein. *J. Cell Biol.* 192:433–445. http://dx.doi.org/10.1083/jcb.201011142